ISSN 2176-5480

22nd International Congress of Mechanical Engineering (COBEM 2013)
November 3-7, 2013, Ribeirão Preto, SP, Brazil

FLOW OVER ROUGH SURFACES

Giulio Dalmolin Cervo
Sérgio Said Mansur
Edson Del Rio Vieira
UNESP – São Paulo State University – Ilha Solteira.
giulio_dm@hotmail.com, mansur@dem.feis.unesp.br; delrio@dem.feis.unesp.br

Abstract. *Flow over rough surface is a common occurrence in nature and subject to many numerical and experimental studies. The rough geometry dictates the flow structure on a mean and instantaneous time scale. In the present work the flow around a flat plate with square and semicircular rough surfaces has been tested in a low turbulence vertical hydrodynamic tunnel for Reynolds numbers up to 2 500. Flow visualized images obtained by direct injection of liquid colored dyes have been captured permitting identify several flow phenomena. Hot film anemometry measurements have been carried out permitting to obtain the non dimension vortex shedding frequency in function of the Reynolds number. Results show a complex dependency of the rough geometry on the flow regime and in the vortex shedding frequency.*

Keywords: *Flow visualization, Vortex shedding, Hydrodynamic tunnel, Rough surface.*

1. INTRODUCTION

After the mid-nineteenth century, with the pioneer works of Hagen – in 1854 – and Darcy– in 1857 –and many others, studies about turbulent flow over rough walls were carried out in order to determine the pressure loss in tubes. Roughness is of fundamental importance for the resistance of turbulent flows internal tubes and channels. In accord to Plandtl and Tietjens, (1934), Blasius and von Mises introduced, only in 1911, the concept of relative roughness using the ratio between the mean height of the roughness irregularities and the tube diameter. Blasius defines that two tubes of different radii have the same relative roughness in case these tubes, for some Reynolds number, give the same friction coefficient value. If two tubes have the same relative roughness, in this sense, the friction coefficient values of both tubes can be represented by a same curve for different Reynolds. Obviously, the resistance of the flow is directly affected not only by the relative magnitude of the roughness irregularities, but also by their geometry.

Hoph (1923) made a comprehensive review of several earlier results about turbulent roughness and found two different roughness surface types in relation to the friction factor. A first roughness kind provokes a loss of pressure approximately proportional to the square of the velocity and a friction factor independent of the Reynolds number and was named “roughness of wall” with roughness irregularities of short wave length and relative high amplitude, as it is shown in Fig. 1(a). Roughness surfaces corresponds to relatively coarse and tightly spaced roughness elements such as coarse sand grains glued on the surface, cement or rough cast iron.

A second roughness type is characterized by long wave length irregularities type waviness, depicted in Fig. 1(b), and named by “waviness wall”.

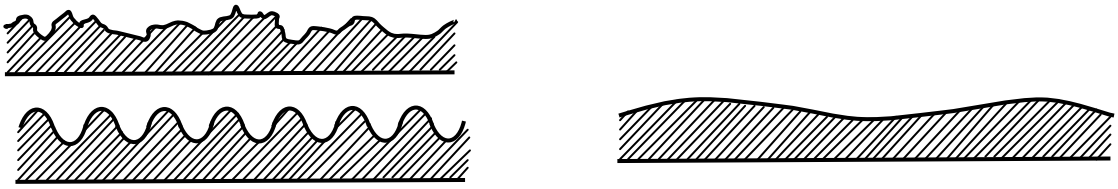

(a) Example of roughness of walls (b) Example of waviness of walls

Figure 1. Types of roughness after Hoph (1923).

In order to explain this two type of roughness, experimental data obtained at that time showed for wall roughness a friction coefficient (f) nearly independent of the Reynolds number (Re) but very dependent of the relative roughness and for waviness surfaces the friction factor can be compared with the smooth tube, as depicted in Fig. 2. A detailed historic review of the flow over roughness surfaces can be found in the thesis of Saleh, (2005).

ISSN 2176-5480

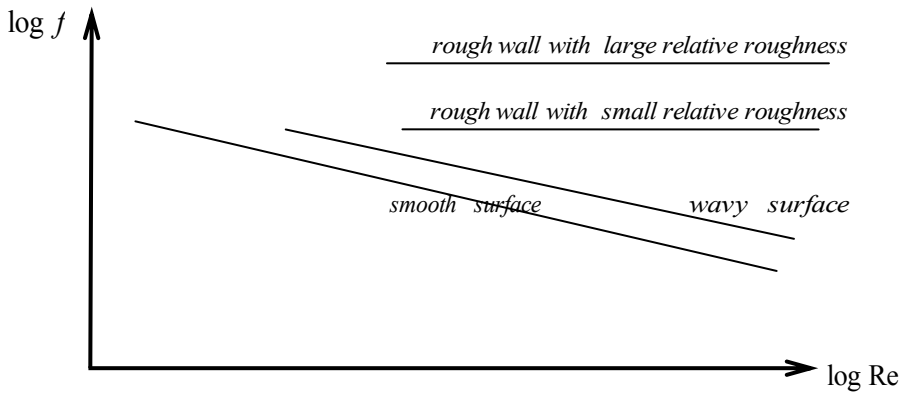

Figure 2. Pressure drop coefficient (f) in tubes and channels with roughness and waviness surfaces.

The studies of Nikuradse in 1933 about the flow internal rough pipes show the influence of the roughness in the mean velocity profile near the wall with modification of the friction coefficient. He utilized circular pipes covered on the inside with sand glued on the wall. By using pipes of varying diameters and by changing the grain size, the relative roughness change from 0.002 to 0.07 and with Reynolds number ranging from 10^4 to 10^6 - (Nikuradse, 1950).

In 1939, "universal" formula of Colebrook for loss of pressure of industrial tubes was proposed. The pioneering work of Nikuradse is the foundation for the Moody diagram, proposed in 1944, for industrial pipes with relatively low values of relative surface roughness. The data of this diagram was developed using sand grains to induce known roughness. Consequently, Moody's diagram is used extensively in predicting friction factors for commercial tubes whose roughness features are not too different from the sand-grain roughness.

In accord to Jiménez, (2004), the distinction between D and K roughness was first made by Perry *et al.* (1969) who was observed that, in several boundary layers over flat plates with narrow square grooves, the effective roughness was not proportional to the roughness height, but to the boundary layer thickness. The limit in which viscosity becomes irrelevant and the effective roughness is proportional only to the roughness dimensions generates roughness surfaces named k – rough or "normal" roughness surfaces, in opposition to the D – roughness. After 1990, the research has emphasized the flow over different types of rough geometries – depicted in Fig. 3 – because small wall details may influence the flow across entire boundary.

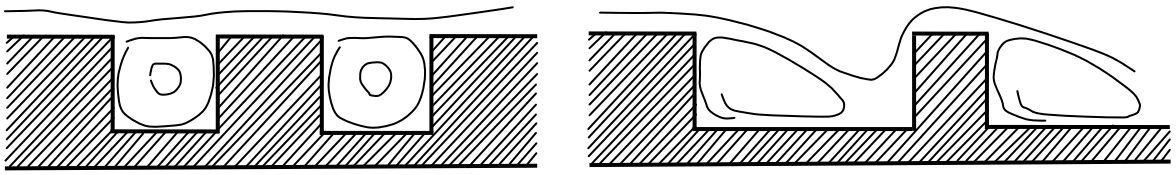

(a) D type roughness surface (b) k type roughness surface

Figure 3. Types of roughness after Perry *et al*. (1969).

The effect of rough walls on turbulent boundary layers is principally controlled by two dimensionless parameters: the roughness Reynolds number and the ratio of the boundary-layer thickness to the roughness height. Roughness is an efficient generator of friction, but this is not an absolute rule, and some moderately rough surfaces reduce drag, for example, in the flow over riblets, we can to observe a decrease drag up to 10% – Sareen, (2012), Mayoral, (2011). Nowadays, a considerable engineering interest has been awakened about turbulent boundary layers over roughness surfaces, principally in moderate Reynolds numbers.

Recently, several new experimental studies of the flow near roughness walls have been performed out in order to provide information about pressure drop, velocity distribution and turbulence flow structures – Molki *et al*. (1993).

Turbulent flows over roughness surfaces are of interest in engineering. Pipes and ducts generally show roughness surfaces, due to economical restrictions in the fabrication process. The presence of roughness may enhance the organization of coherent flow structures in the turbulent boundary layer, principally the formation and shedding of vortices. Several organized flow structures near the wall can be observed in the flow over roughness surfaces and they are responsible for heat, mass and momentum transfer across the turbulent boundary layer.

ISSN 2176-5480

In this present work, the flow over a flat plate with square and semicircular rough surfaces has been carried out in a vertical hydrodynamic tunnel in Reynolds number – based in the rough irregularities height – up to 2 500. Using flow visualized images, in a qualitative view point, several flow structures near the wall can be identified in different Reynolds number. Additionally, quantitative hot film anemometry data allow determining the vortex shedding frequency produced by the roughness irregularities. Figure 4 depicts the two geometries of roughness tested in the present work.

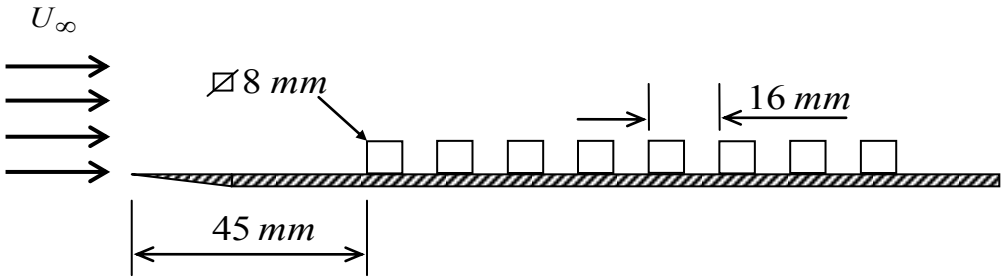

(a) Square roughness surface

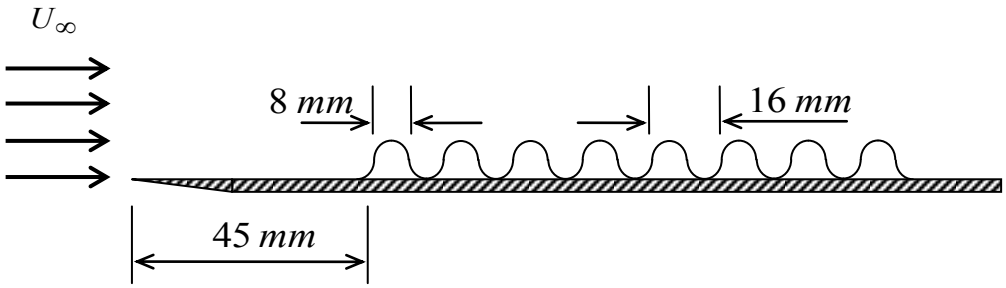

(b) Semicircular roughness surface

Figure 4. Roughness surfaces tested.

2. VISUALIZED IMAGES OF THE TWO DIMENSIONAL FLOW OVER ROUGH SURFACES

Surface roughness modifies the near-wall flow by generating additional vortex structures in the wake region of the roughness elements and enhances the turbulence production. These turbulent phenomena can be characterized from the natural shedding frequency of vortex structures. Many experimental works have been carried out in order to throw light on the flow structures formed in turbulent flow over roughness surfaces with different geometries by means of several techniques. Different quantitative measurements using sample techniques can be used in order to detect coherent structures from velocity fluctuations. Flow visualization studies have been demonstrated the vortex shedding phenomena of the flow over flat roughness surfaces. In a qualitative sense, flow visualization of streaky patterns with help of passive tracers can be carried out permitting detect several flow structures. For many years, turbulence was considered as a completely random phenomenon, but flow visualization of Kim *et al*. (1971), Brown and Roshko (1974) and others have showed the importance of coherent structures in turbulent flows. After this, turbulence is now viewed from a more deterministic view point. Since Leonardo da Vinci, the flow visualization tools are intensively utilized in order to understanding the complex phenomena associated with the fluid motion. Today, despite of strong development of modern flow velocity measurement systems, flow visualization techniques remain as a useful research tool to identify the large turbulent flow structures.

Flow visualization studies have demonstrated shedding of vortices from roughness elements. It is common to express the vortex shedding in terms of Strouhal number, based on the mean time period of vortex shedding. Djenidi *et al*. (1998) performed experimental visualization, using Laser Induced Fluorescence (LIF) technique, of the flow over a wall with square cavities placed transversally to the flow direction and spaced one cavity apart in x direction. Sodium fluorescein and Rodamine® dyes have been injected through a spanwise slot and illuminated by a laser sheet of 0.5 mm of width. In the work of Djenidi *et al*. (1998) the vortex shedding phenomenon is observed, but no measurement of the vortex shedding frequency was performed.

A better knowledge of the turbulence structure of the flow over roughness surfaces is necessary to validate and improve numerical simulations, particularly to atmospheric boundary layer which are usually rough. In this sense, the work of Tomas *et al*. (2011) shows an experimental study using a vertical large water flume (22 m long, 3 m wide and

ISSN 2176-5480

1 m high). The roughness element are constituted by conventional LEGO® blocks and PIV and LDV measurements has been carried out in order to verify the boundary layer growth.

Laadhari *et al*. (1994) carried out experiments in a wind tunnel (6 m long and 0.5 ×0.5 m wide) using flow velocity and wall pressure measurements and flow visualization by smoke injection in a boundary layer. Combination of qualitative flow visualization and quantitative measurements provides useful information about transition. Coherent structures identified by flow visualized images are related to pressure wall and velocity fluctuations.

In other side, the experiments conducted by Bandyopadhyay and Watson (1988) estimated the time period vortex shedding in a rough wall with square protuberances in two ratio of span to height of a roughness element – spanwise aspect ratio. D or k rough surface was obtained only utilizing two spanwise aspect ratios.

Leonardi *et al*. (2003) show an important two dimensional Direct Numerical simulation of the fully developed turbulent channel flow with a wall with square bars separated by a rectangular cavity for Reynolds, based in the height of the channel, $Re = 4200$ showing a strong influence of the blockage ratio on the streamline. Same results obtained by Bassan (2011).

In all of these works, the use of flow visualization allows to identify several important large turbulent flow structures. In the present work, the flow images obtained by liquid dye injection techniques of the flow over roughness surfaces with square and semicircular protuberances have been captured and several flow structures have been identified.

3. EXPERIMENTAL APPARATUS

All experiments have been carried out in a vertical open circuit hydrodynamic tunnel with a 146×146×500 mm square cross test section operated by gravitational action. Several modifications have been carried out in the hydrodynamic tunnel extending its operational envelope up to 2 m/s. Boundary layer thickness effect on velocity profile is controlled by divergent walls in the test section showing an adequate solution. All tests were run over the Reynolds number range (*Re*), based on approach flow velocity (*V*) and roughness height up to 2,500. The hydrodynamic tunnel is operated by gravitational action, and can be used in continuous or blow-down mode. Blow-down or intermittent mode has been used in this work in order to obtain the flow visualized images and continuous mode in the measurement of the vortex shedding frequency. The free flow velocity has been determined utilizing a Yokogawa electromagnetic flowmeter ADMAG AXF100G. The uncertainty in the free flow velocity determination is estimated in less than ±3%, producing a maximum uncertain less than 5% for the Reynolds number. For further information on the water tunnel characteristics, reference may be made to Bassan *et al*. (2011a,b).

In the present work, the free stream turbulence level was measured in the center line of the test section with the hydrodynamic tunnel operating in continuous mode. In all measurements the velocity signal was obtained with an acquisition rate of 13 kHz in blocks with 131,072 points each. Turbulence level is calculated utilizing RMS procedure. With the tunnel operating in blow-down mode the relative turbulence level is approximately twice times less than the turbulence for continuous mode, in accord to shown in Fig 5. Fig. 6 depicts the velocity profile in the test section for 5 different velocities.

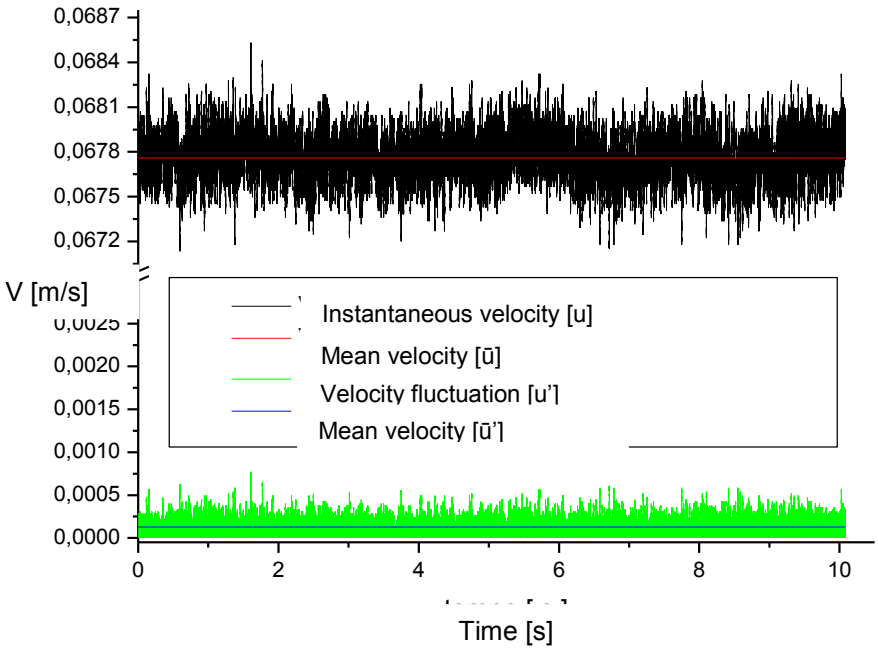

Figure 5. Free turbulence measurement in the test section.

ISSN 2176-5480

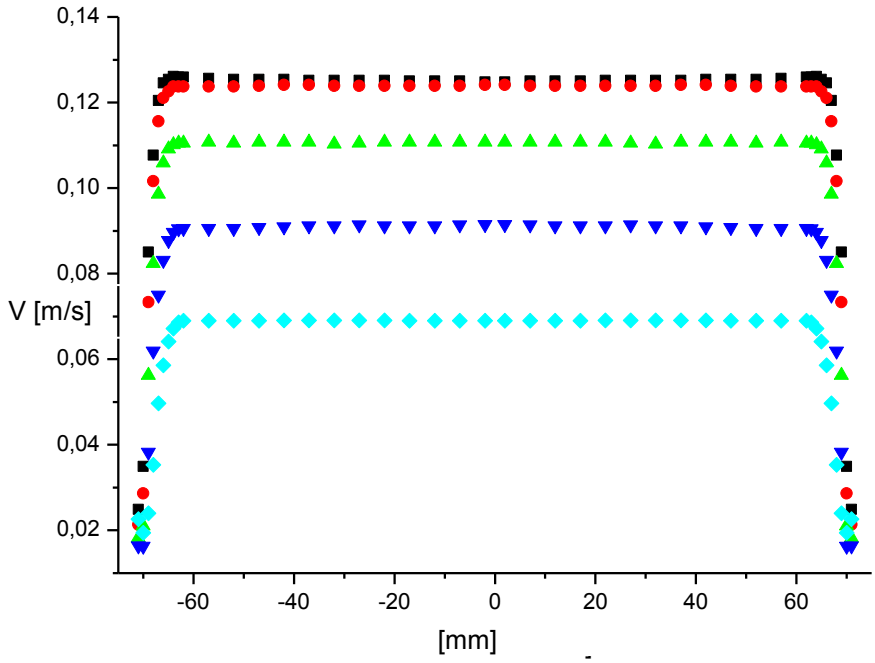

Figure 6. Velocity profile in the test section.

The flow visualization technique applied in the present work is the direct injection of opaque liquid dye in non-perturbed flow by means a rake of long hypodermic needles of 0.7 mm O. D.. The dye utilized is a solution of colored PVA pigments, water and ethyl alcohol. Ethyl alcohol is only to correct the solution density very close to water. If occurs density difference between the dye solution and water, in very low Reynolds number, undesirable effects of convection is visible. Strong amount of this colored dye has been injected directly in the non perturbed stream, sufficient to color the entire flow field. Subtly, the injection dye is stopped, and the clean water flow wash the entire flow field, except in the cylinder wake, because in this region the flow speed is significantly small than other regions. This procedure permits to see, for seconds, the re-circulating bubble and the wake downstream the cylinder.

Still images are also captured using a 12.3 megapixel *Nikon* D 90 DSLR single lens reflex camera equipped with a special *Nikkor* medical macro lens with 120 mm and f/1:4. The pictures have been obtained in f/1:11 and 1/250 s for ISO 100. Cold illumination by means of day light fluorescent lamps with high color temperature (5,500 K) but minimal heat emission and high frequency (5,000 Hz) has been adapted in the tunnel permitting sharp and well defined images. The use of Rosco diffuser Cinegel#3007, a slight filter with less density softens edge, provides a good illumination for still and video image capture.

In all experiments was utilized the 55R11 fiber-film probe made by *Dantec Measurement Technology*, with 70 μm diameter quartz fiber coated with 2 μm nickel film and with an overall length of 3 mm. This is a straight general-purpose type sensor which permits a wide measurement range in water medium. For very small velocities (up to 0.10 m/s) several special cares could be observed in order to reduce the convection effect around the probe. A *Dantec StreamLine* 90C10 frame with 3 CTA modules 90C10 permits simultaneously measurements in 3 channels. An A/D board NI-DAQmx 8.7.1 (16 bits), made by *National Instrument,* has been utilized in order to record the output voltage signal.

4. RESULTS

Figure 7 shows images of flow over a flat plate provided with square (a) and semicircular (b) protuberances positioned perpendicular to the main flow. Flow patterns at relatively low Reynolds number, near creeping flow, show a very little detachment for square protuberances with the dye streaklines skirting almost perfectly the solid obstacles. In opposition, for semicircular roughness, the dye streaklines flow no show relative appreciable detachment.

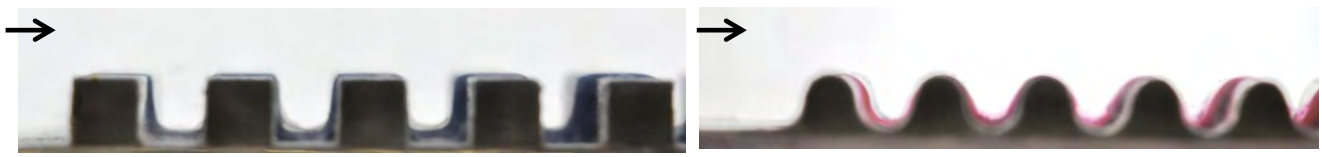

(a)Square protuberances Re ≈ 11 (b)Semicircular protuberances Re ≈ 10

Figure 7. Flow visualized images of the roughness surfaces in relative low Reynolds number.

ISSN 2176-5480

An appreciable detachment is possible to visualize in Reynolds number higher like showed in Fig. 8. An increase of the velocity causes boundary layer detachment in the first protuberance and is possible to observe three distinct regions within each cavity. The first region is formed by a clockwise vortex that occurs due to the difference in speed between the low speed and the main flow inside the cavity. The second is the region that extends from the lower left corner to the upper left corner where it is not possible to view the presence of dye, since this was washed by the movement of the fluid. It can be argued that this region has a recirculation counterclockwise since their movement should be opposed to the first region, as illustrated in Fig. 9. The third region is a large concentration of dye at the bottom right of the cavity. In this region, the fluid velocity is extremely low; and the dye remains visible for a longer period of time than in other areas of the cavity.

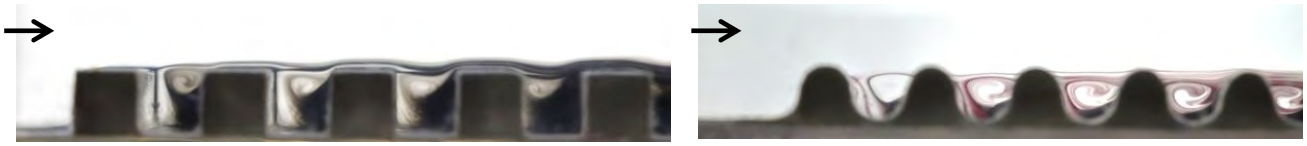

(a)Square protuberances Re ≈ 35 (b)Semicircular protuberances Re ≈ 40

Figure 8. Flow visualized images of the roughness surfaces in relative low Reynolds number.

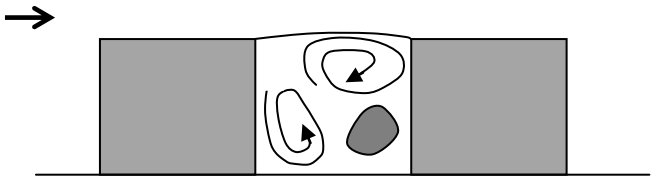

Figure 9. Flow recirculations internal the cavity.

An increase of the Reynolds provokes an increase of the clockwise vortex recirculation size and decrease of the under clockwise recirculation size. In Fig. 10 is possible to visualize the clockwise recirculation with dimensions very close to the cavity dimensions. This situation is possible to be observed in Fig. 11. But, for a square protuberance and Reynolds equals to 228 - Fig. 11(a) –, the detachment occurs in the top left corner of the first protuberance. For Reynolds less than 228 the detachment occurs in the top right corner and a reattachment has been possible to observe in the top of the next protuberance. For Reynolds more than 228 the reattachment no more is observed. In Re = 321 (Fig. 12) for square protuberance we can observe a formation of several complex recirculation structures, depicted in Fig. 13. For semicircular protuberances these large turbulent structures formation no are observed.

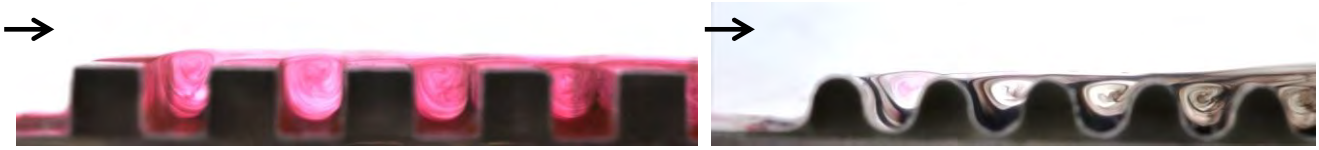

(a)Square protuberances Re ≈ 134 (b)Semicircular protuberances Re ≈ 147

Figure 10. Flow visualized images of the roughness surfaces.

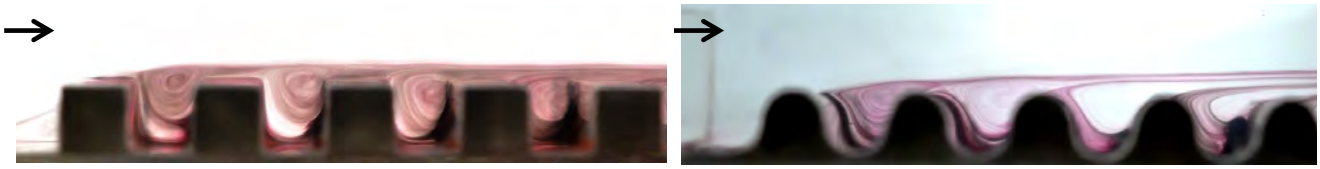

(a)Square protuberances Re ≈ 228 (b)Semicircular protuberances Re ≈ 215

Figure 11. Flow visualized images of the roughness surfaces.

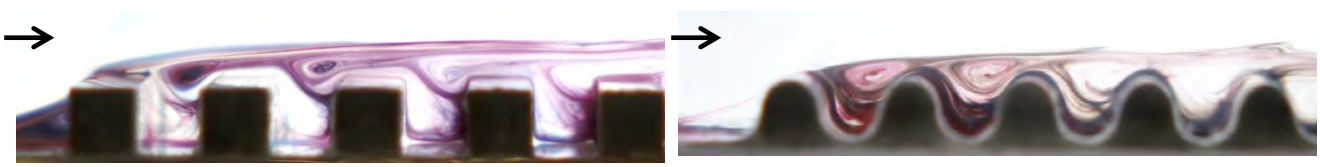

(a)Square protuberances Re ≈ 321 (b)Semicircular protuberances Re ≈ 338

Figure 12. Flow visualized images of the roughness surfaces.

ISSN 2176-5480

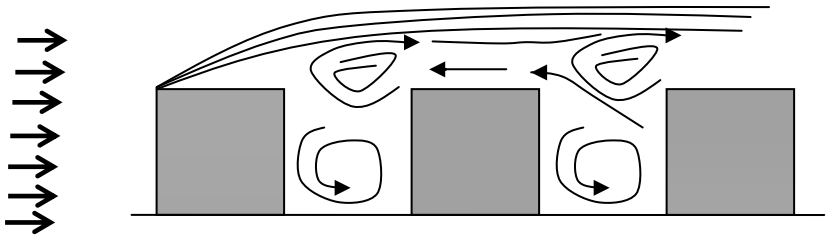

Figure 13. Sketch of the recirculation produced in square roughness surface external the cavities - Re = 321.

These turbulent structures are only observed in square protuberances, probably due to existence of a sharp edge in the top of the square protuberances producing a boundary layer detachment and the formation of stable recirculation external the cavities. The vortex formation and shedding can be observed in Fig. 14 for several Reynolds numbers.

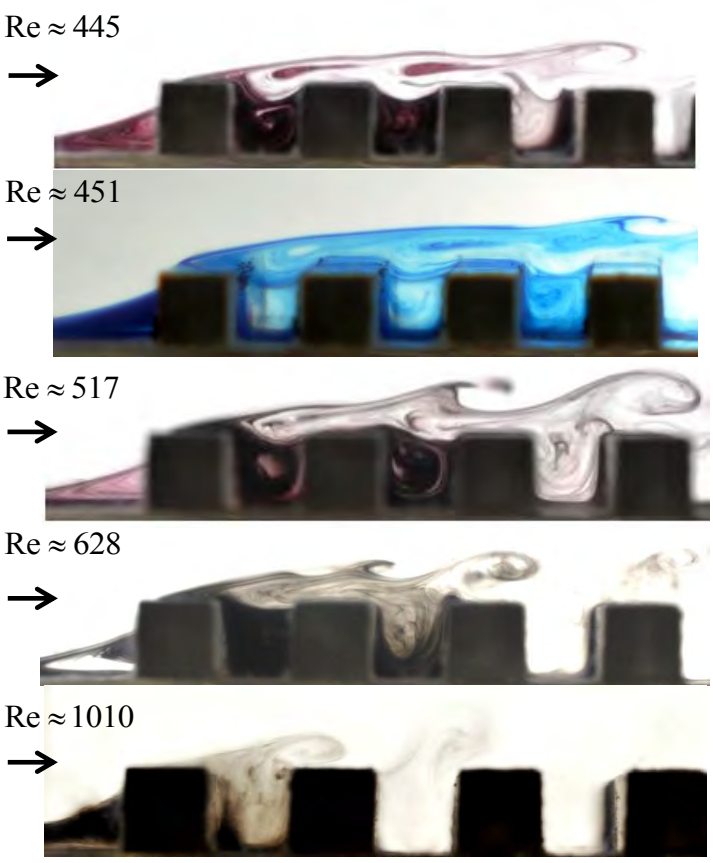

Figure 14. Vortex shedding in square protuberances.

For semicircular protuberances, the formation of large recirculating structures is also observed, as showed in Fig. 15. The visualization and identification of eddy structures become increasingly difficult as the increased fluid velocity in the test section. The flow over square protuberances - Figure 14 - shows morphologic aspects with a relative similarity with the flow over semi circular obstacles, shown in Fig 15.

Measurements of the vortex shedding frequency have been carried out utilizing hot film anemometry. The hot film probe was adequately positioned in the flow as can be visualized in Fig. 16. As an example, Figure 17 shows the temporal velocity signal and the frequency spectrum obtained in a test performed for Re = 946. The digital signal obtained is shown in Figure 16 (a), where the electrical output voltage variation is recorded as a function of time. In order to obtain the Strouhal number that characterizes the phenomenon of emission of vortices has been applied to fast Fourier transform (FFT) in the acquired digital signal, thus producing the frequency spectrum shown in Fig 17 (b).

ISSN 2176-5480

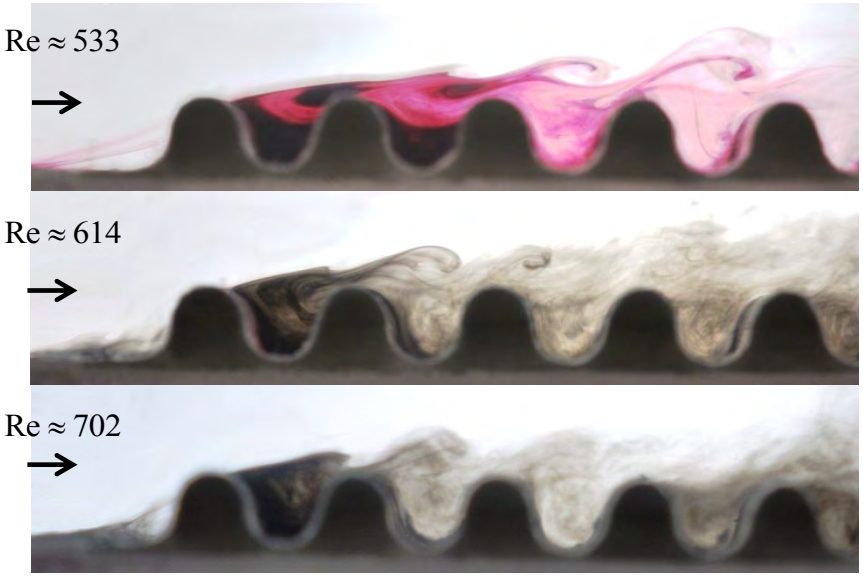

Figure 15. Evolution of the flow structures in semicircular protuberances.

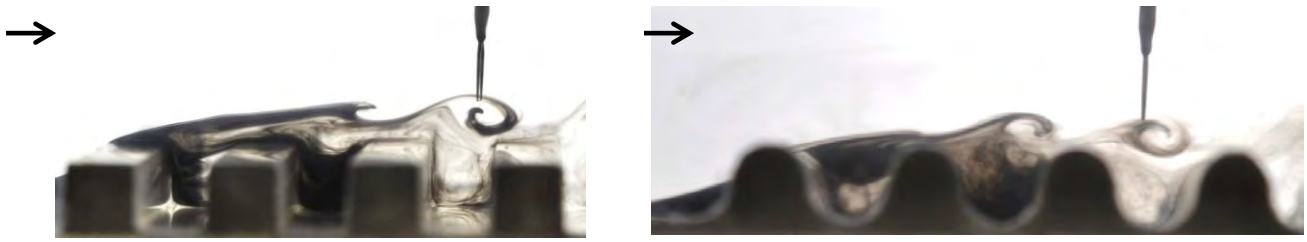

Figure 16. Hot film probe positioning in the third cavity.

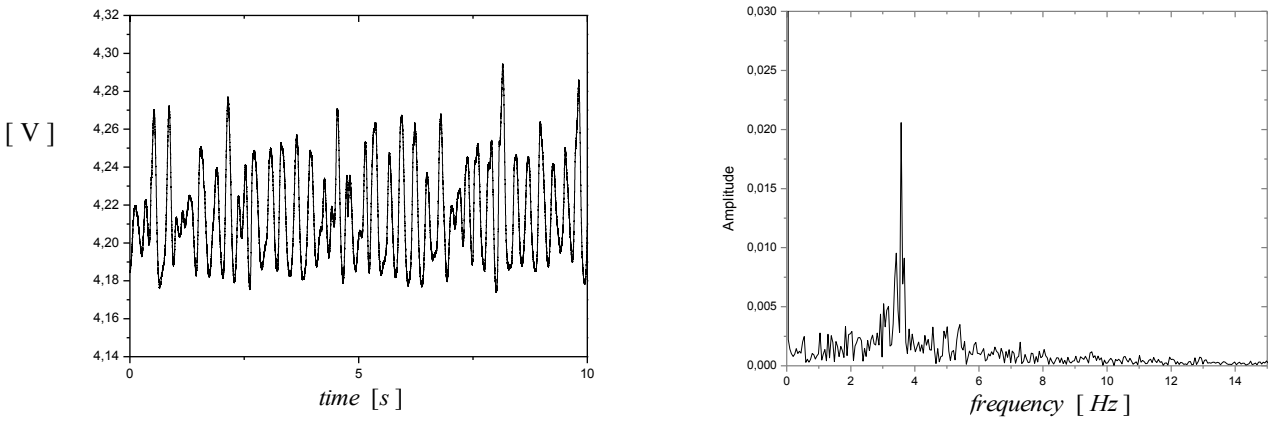

(a) Temporal velocity (b) Frequency spectrum

Figure 16. Hot film velocity acquisition for Re = 946 with square protuberances.

In order to investigate the vortices emission frequency, several tests were carried out for different values of Reynolds number. Fig. 17 shows the vortex frequency for square protuberances. In the range of Reynolds number between 445 and 1600, one in which the velocity increase is proportional to the increase of the vortex shedding frequency. This linearity is maintained for Reynolds increase; however we can observe two discontinuities that occur for Reynolds numbers approximately equal to 1,600 to 2,000. This phenomenon occurs because a new flow pattern is developed and the frequency of vortex shedding is suddenly increased and then decreased. Several new tests have been performed out in order to verify the influence of the probe positioning in the vortex shedding frequency. Fig. 18 shows the vortex shedding frequency obtained in two probe position: over the third cavity (as showed in Fig. 16) and over the first square protuberance. No appreciable difference has been observed in the vortex shedding frequency due to probe positioning. Fig. 18 also shows the study of influence of probe support geometry in the vortex shedding frequency. The probe support has a bluff geometry which produces vortices and consequently generates probe oscillations. Two

ISSN 2176-5480

different new geometry of probe support have been test in order to verify the influence of vortex shedding from probe support in the vortex shedding frequency produced by roughness surface. A first geometry is an aerodynamic hood – showed in Fig. 19 (a) positioned over the first protuberance - and the second new probe support geometry is a relatively large diameter cylinder hood – showed in Fig. 19(b) over the third protuberance. In all tests performed out no appreciable interference of the probe support geometry has been observed on vortex shedding frequency obtained. Finally, Fig. 20 shows a vortex shedding frequency for semicircular protuberances.

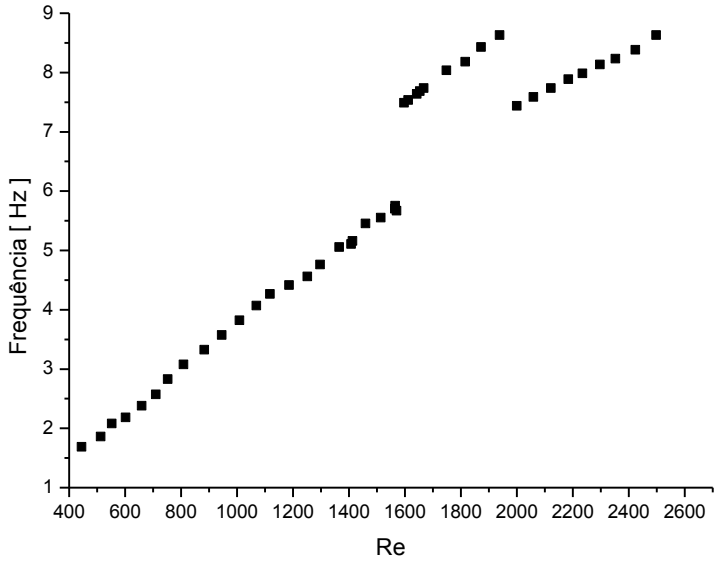

Figure 17. Vortex shedding frequency in a square roughness surface.

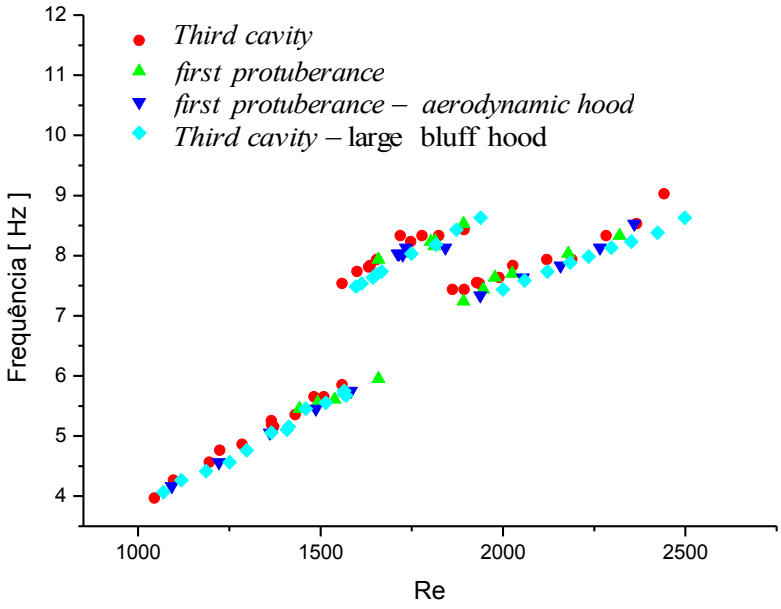

Figure 18. Vortex shedding frequency in function of Reynolds number in a square roughness surface for two different probe positions and probe support.

ISSN 2176-5480

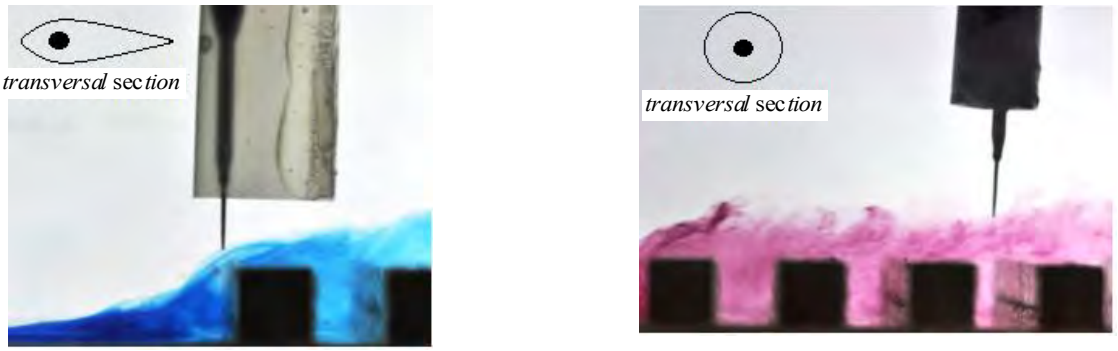

(a) Aerodynamic hood probe support (first rough) (b) Large bluff body probe support (third cavity)

Figure 19. Two different probe support geometries tested.

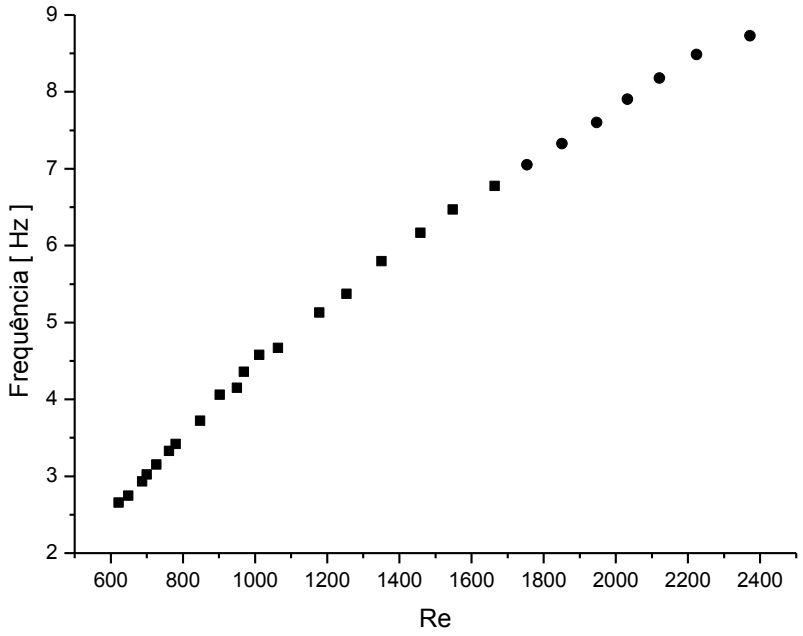

Figure 20. Vortex shedding frequency obtained for semicircular roughness.

5. CONCLUSIONS

Effects of turbulent flow over roughness surfaces have been experimentally studied since the mid-nineteenth century. A better knowledge of the large scale turbulent structures of the flow over roughness surfaces is necessary in order to validate and improved numerical studies. In the case of atmospheric boundary layer, which is a usually roughness surface, have also received attention of several studies. In the present work, square and semicircular geometries of protuberances have been tested in order to obtain the flow images and vortex shedding frequency in moderate Reynolds numbers. Tests for vortex shedding frequency have been performed out for Reynolds up to 2,500. Unfortunately, the liquid dye injection technique employed in this present work generates imprecise images with a low definition for Reynolds more than 1,000 due to relative high velocity of the tests. New flow visualization techniques should be tested in order to obtain clear images of the flow for more elevated Reynolds numbers.

The flow over the two types of geometry – square and semicircular protuberances – shows a closed similarity for Reynolds less than 1,000. For more elevated Reynolds number, square roughness shows a sensible discontinuity in the vortex shedding frequency. Strouhal discontinuity has been no observed in the tests of the semicircular roughness in the range of Reynolds tested.

Strouhal number discontinuities were also found in the flow around several bluff body cylindrical geometries without wall interference. Lindquist *et al*. (1998), for an isolated rectangular cylinder with 2:1 aspect ratio (the ratio of the streamwise length to width ratio), found a discontinuity at a range of Reynolds between 450 and 550. The behavior of the Strouhal number of rectangular cylinders with different ratios was also subject to experimental and numerical

ISSN 2176-5480

studies of Okajima (1982) with the same occurrences of discontinuities obtained by Lindquist *et al*. (1998). For rectangular cylinders the Strouhal discontinuity are due to boundary detachment and re-attachment process. For an isolated square cylinder (aspect ratio 1:1) with a low blockage ratio (i.e. far the wall interferences) Lindquist *et al*. (2010) observed a Strouhal number discontinuity due to change in the attack angle in a constant Reynolds number. In this case, for Reynolds constant, the cylinder rotation changes the attack angle and, consequently boundary layers detachment and re-attachment occurs due to the relative position of the sharp corner of the square cylinder in relation of the flow direction. In the present work, sharp edge of the square protuberances provokes intense detachment of the boundary layer, observed in the Fig. 10(a) in the second edge of the first protuberances for Re=134. For more elevated Reynolds numbers - Re=321 -, showed in the Fig. 12(a), the detachment changes to the first corner of the first protuberances and, in this case, no is observed the re attachment in the top surface of the first protuberance.

Probably, the nonexistence of sharp edges in the semicircular roughness is responsible to a continuous Strouhal Reynolds curve without discontinuous. But, a conclusive answer to this complex question about Strouhal discontinuity of square roughness surface depends of many others tests.

6. ACKNOWLEDGEMENTS

The authors are grateful to the financial support provided by FAPESP (Fundação de Amparo à Pesquisa do Estado de São Paulo) and also thankful for CAPES/CNPq, FUNDUNESP and FEPISA for supporting the construction and acquisition of the experimental apparatus used in this study.

7. REFERENCES

Bandyopadhyay, P.R. and Watson, R.D., 1988, "Structure of roughwall turbulent boundary layers", Physics of Fluids, vol. 31, pp. 1877-1883.

Bassan, R.A., 2011, "Experimental visualization of the flow internal a channel with square bars" (in Portugueese) MsC dissertation, Unesp-Ilha Solteira.

Bassan, R.A., Mansur, S.S. and Vieira, E.D.R., 2011. "Rebuilt of a vertical hydrodynamic tunnel". *Proceedings of the 21st Brazilian Congress of Mechanical Engineering* – COBEM, Natal, RN, Brazil.

Bassan, R.A., Mansur, S.and Vieira, E.D.R., 2011. "Experimental Flow Visualization Internal Channels with Wall Protuberance" (in Portuguese), *Proceedings of the CIBEM 2011 – 10º Congresso Iberoamericano de Engenharia Mecânica*, Porto, Portugual.

Brown, G.L. and Roshko, A., 1974, "On density effects and large structure in turbulent mixing layers", Journal of Fluid Mechanics, Vol 64, pp.775-816.

Djenidi, L; Elavarasan, R. and Antonia, R.A., 1998, "Turbulent boundary layer over transverse square cavity". *In: Proceedings of the 13th Australasian Fluid Mechanics Conference*, Melbourne, Australia.

Hopf, L., 1923, "The measurement of the hydraulic roughness" (in German) Mathematik und Mechanik, vol. 3, pp.329-339.

Jiménez, J., 2004, "Turbulent flows over rough walls". Annual Review of Fluid Mechanics, vol. 36, pp. 173-196.

Kim, H.T.; Kline, S.J. and Reynolds, W.C., 1971, "The production of turbulence near a smooth wall in a turbulent boundary layer", Journal of Fluid Mechanics, Vol. 50, Part 1, pp.136-160.

Laadhari, F.; Morel. R and Alcaraz, E., 1994, "Combined visualisation and measurements in transitional boundary layers", European Journal of Mechanics, B/Fluids, Vol. 13, nº 4, pp.473-489.

Leonardi, S.; Orlandi, P.; Smalley, R.J.; Djenidi, L. and Antonia, A., 2003, "Direct numerical simulations of turbulent channel flow with transverse square bars on one wall", Journal of Fluid Mechanics, vol. 491, pp.229-238.

Lindquist, C.; Mansur, S.S. and Vieira, E.D.R., 1998, "Experimental study of the flow around rectangular cylinders: An application to compact heat exchanbers" (in Portugueese). In: *Proceedings of the* 8st *Brazilian Congress of Thermal Science and Engineering*, Rio de Janeiro, RJ, Brazil.

Lindquist, C.; Mansur, S.S. and Vieira, E.D.R., 2010, "Flow around square cylinders in several attack angles". In: *Proceedings of the* 13st *Brazilian Congress of Thermal Science and Engineering*, Uberlândia, MG, Brazil.

Mayoral, R.G., 2011, "The intercation of riblets with wall-bounded turbulence", Ph.D. Thesis, Universidad Politecnica de Madrid, 119 p.

Molki, M.; Fahri, M. and Ozbay, O., 1993, "A new correlation for pressure drop in arrays of rectangular blocks in air cooled electronic units", ASME HTD, vol. 237, pp. 75-81.

Nikuradse, J., 1950, "Laws of flow in rough pipes", NACA Technical Memorandum TM 1292, translation of the "Strömungsgesetze in rauhen Rohren", VDI –forschunesheft, 361, 1933.

Okajima, A., 1982, "Strouhal numbers of rectangular cylinders", Journal of Fluid Mechanics, vol. 123, pp. 379-398.

Perry, A.E.; Schofield, W.H. and Joubert, P., 1969, "Rough wall turbulent boundary layers", Journal of Fluid Mechanics, vol. 73, pp. 383-413.

Prandtl, L. and Tietjens, O.G., 1934, "Applied Hydro-and Aeromechanics", General Publishing Company, Ltda, Toronto, Canada.

Saleh, O.A.B., 2005, "Fully developed turbulent smooth and rough channel and pipe flows", Ph.D. Thesis, Erlangen-Nürnberg University, 116 p.
Sareen, A., 2012, "Drag reduction using riblet film aspplied to airfoils for wind turbunes", Ph.D. Thesis, University of Illinois at Urbana-Champaign, 237 p.
Tomas, S.; Eiff, O. and Masson, V., 2011, Experimental investigation of the turbulent momentum transfers in a neutral boundary layer over a rough surface", Boundary-Layer Meteorology, vol. 138, pp.385-411.

8. RESPONSIBILITY NOTICE

The authors are the only responsible for the printed material included in this paper.